Chapter 16

Biofuels in Aircraft Engines

Anna Maiorova, Aleksandr Vasil'ev and Oganes Chelebyan

Additional information is available at the end of the chapter

http://dx.doi.org/10.5772/59871

1. Introduction

A large number of studies conducted in Russia and abroad have been devoted to the development of low-emission gas turbine engines for aircraft and power stations (see, e.g., [1]). However, the continual improvement of the environmental requirements of ICAO (International Civil Aviation Organization) forces new research to be carried out.

The use of renewable biofuels obtained from plants or fatty acids is very promising. At present, aviation accounts for about 2% of man-made emissions of CO_2 [2]. When using biofuel, the emission of smoke, solid carbon, carbon monoxide, sulfur and total carbon dioxide is decreased. The most economically feasible is a fuel that can be mixed in any proportion with conventional jet fuel and does not require the creation of an alternative ground fuel-supply infrastructure and ad hoc adjustment of aircraft engines. Thus, the use of bio-kerosene obtained from jatropha, instead of the traditional kerosene in aircraft would reduce "carbon trace" almost by 80%.

Fuel	Density, kg/m³	Kinematic viscosity $\cdot 10^6$, m²/s	Surface tension coefficient $\cdot 10^3$, N/m	Calorific value, M j /kg
Ethanol	788	1.550	22.3	27.2
Kerosene TS1	≥780	≥ 1.3	24.3	43.3
Summer diesel	≤ 860	3.0-6.0	28.9	42.5
Winter diesel	≤ 840	1.8-5.0	27.8	42. 5
FAME (biodiesel)	877-879	8.0	31.4	37.5
Vegetable oils	870-960	51-110	24.8 - 34.4	37 - 42.5

Table 1. Physical properties of fuels at 20°C

Foreign companies in recent years (2008-2014) have been intensively studying the possibility of using alternative fuels without the need for modification of aircrafts and engines. The first flight of the airplane on biofuel took place in 2008. The British Airline Virgin Atlantic Airways Ltd is the proprietor of that aircraft. Boeing and its international partners are already working hard to bring biofuels from the testing stage to the manufacturing stage. Boeing 747-8 Freighter and the 787 Dreamliner made the first demonstration of transatlantic and transpacific flights on biofuels in 2011 and 2012 [3]. In May 2014, KLM began weekly flights by an Airbus A330-200 between Queen Beatrix International Airport, in Oranjestad, Aruba, and Amsterdam's Schiphol Airport, Netherlands, using converted cooking oil as aircraft fuel [4]. So far, Russia has not done commercial-scale biofuel production. However, this trend has a great future because of the presence of large sown areas and water surfaces in our country [5]. Within the framework of the International Aviation and Space Salon MAKS-2013 Airbus and Rosteh State Corporation signed a partnership agreement in the field of aviation biofuels in Russia using only renewable resources.

One can find a large number of articles devoted to biofuels in the world literature (e.g. [6], [7]), a number of articles in [8]). An overview of current studies of the structure of such fuels as well as the characteristics of the processes of combustion and pollutant emissions in various types of engines is given in [9]. However, vast majority of the work are carried out in relation to internal-combustion engines or diesel engines. Studies on the atomization and combustion of biofuels compared with petroleum fuels in relation to gas turbine engines, as well as designing multi-fuel combustion chambers in the press are virtually absent. Nevertheless, one can see from Table 1 (the physical properties of various fuels corresponding to the Russian and international standards [10- 13]) that the spread in values of the fuel properties is rather wide, especially for viscosity. The present work is a continuation of researches [14] and [15]. In research [14] the design, manufacture and test of individual injectors and the burner as a whole for low-emission combustion chambers of gas-turbine engine or gas-turbine plant have been executed. Results showed that the designed spray unit can be used for different liquid fuels, both for fossil and for alternative fuels. The present work is devoted to the study of the influence of the physical properties of conventional fuels and biofuels on the characteristics of fuel–air aerosols and the combustion process. Fuel spraying was carried out by means of the developed burner.

2. The peculiarities of atomization of liquid fuels with different physical properties.

Experimental studies of the features of fuel–air sprays were performed at the Central Institute of Aviation Motors using laser diagnostics setup. The description of the test bench is given in reference [15]. The setup is equipped with instruments for laser measurements of the quality of spraying and the rate of droplets by the light scattering. In this work, the physical studies were carried out using the method of Phase-Doppler anemometry (PDPA TSI, United States). Digital photography was carried out using a Canon XL_H1 three-matrix color camera-recorder (Japan). As an object of study, a double-channel fuel burner with combined centrifugal-airblast

http://dx.doi.org/10.5772/59871

design was chosen [16]. The scheme of the spraying device is shown in Fig. 1. The channels of the nozzles are arranged concentrically. A pressure swirl pilot channel with a low rate of flow and cylindrical outlet nozzle is mounted on the burner axis. The main fuel feed channel is airblast with a ring nozzle. It is placed between the two air swirlers for better atomization of the liquid film and for stabilization of the fuel–air spray. The angles of the vane inclination of inner and peripheral swirlers relative to the axis of the device were 60° and 45°. The outer diameter of the fuel nozzle in a pneumatic atomizer is 22 mm and 1.1 mm in a centrifugal atomizer. A detailed description of the burner is given in [14], where it was tested on various petroleum and alternative fuels.

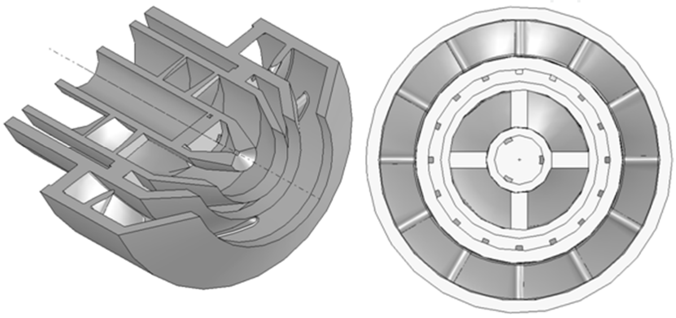

Figure 1. Test object

In this section, we studied the atomization at normal conditions for three types of liquid: (1) water (kinematic viscosity $\nu_F = 1.05 \times 10^{-6}$ m^2/s, surface tension $\sigma_F = 73 \times 10^{-3}$ N/m), (2) kerosene ($\nu_F = 1.9 \times 10^{-6}$ m^2/s, $\sigma_F = 25 \times 10^{-3}$ N/m), and (3) a mixture of diesel fuel with rapeseed oil in the ratio of 50 : 50 ($\nu_F = 13.7 \times 10^{-6}$ m2/s, $\sigma_F = 30 \times 10^{-3}$ N/m), which imitated liquid biofuel.

We used three methods of spraying: hydraulic (in which the energy of the liquid is used for spraying), pneumatic (spraying of liquid in the flows of air), and a combined centrifugal-pneumatic process, in which liquid spraying occurs due to the of the liquid state's own energy and the energy of air.

The first stage in the research on the atomization process is the investigation of the decomposition of liquid fuel films due to the loss of their own stability (hydraulic atomization). Figures 2–6 show the results of this investigation.

The results of this series of experiments allow us to make some assumptions about the mechanism of the liquid film decay into droplets. The film of the fuel is formed as a result of the interflow of swirled liquid streams into a single stream along the length of the swirl chamber and the nozzle of the injector. In this case, one can assert that when the fluid moves through the caves of the injector, its outer layer is decelerated due to the friction with the surface and the velocity components diminish in this layer. This gives rise to the shear stresses along the fuel film thickness. We can assume that with an increase in the velocity, depending on the properties of the fluid and geometrical parameters of the atomizer, the shear of the layers becomes so significant that the outer sublayer is swirled in the opposite direction relative to the velocity vector (the scheme is shown in Fig. 2). At the exit of the nozzle, after sudden

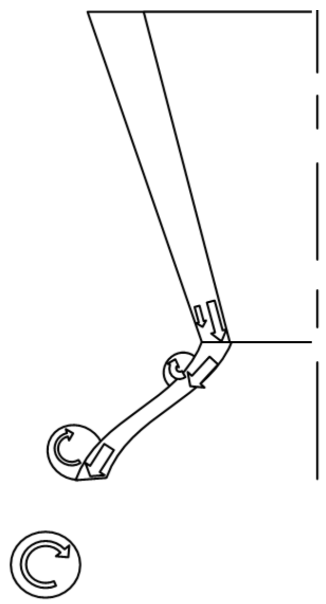

Figure 2. Scheme of the formation of waves–vortexes on the surface of the liquid film

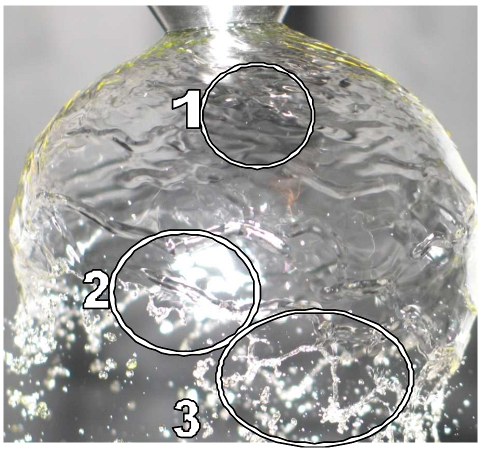

Figure 3. Development and decay of the waves upon hydraulic spraying of kerosene through an annular nozzle (photo) at G_F =17.5 g/s, G_A = 0

expansion and separation from the surface, the intensity of the vortex increases rapidly and waves are formed. When moving downstream, the wave height above the level of the film increases (see markers *1* and *2* in Fig. 3). The growth of these waves is caused by the fact that swirled formations move in the axial direction with lower velocity than the film and then disintegrate into bundles and individual droplets at a certain moment when capturing additional mass (marker 3 in Fig. 3). Such a vortex structure of the waves is confirmed by a series of images shown in Fig. 4, where we can clearly see that a sufficiently large number of droplets deviate from the direction of the stream outwards from the film at various expiration velocities and different nozzle designs. This can be explained by the disintegration of the swirling roller of the fluid as it moves in the direction backward to the main flow, and the roller (or its components) deviates to the periphery of the burner.

http://dx.doi.org/10.5772/59871

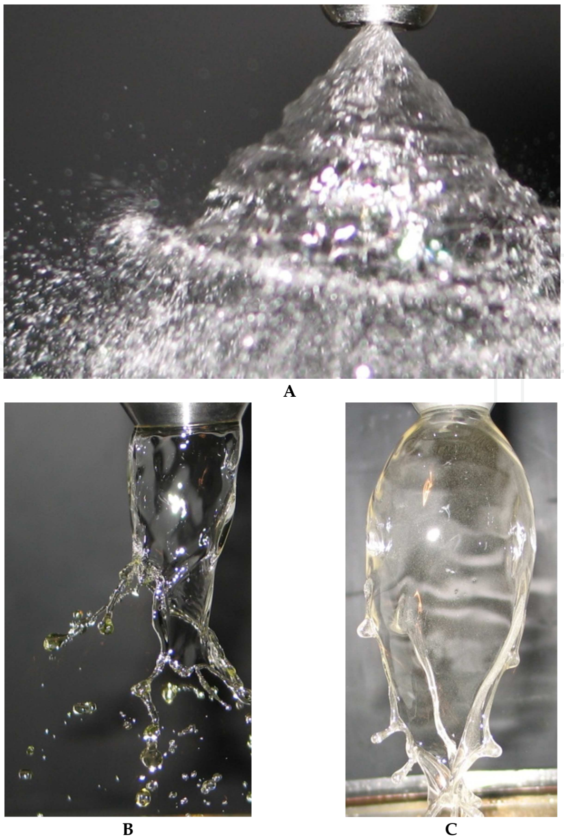

Figure 4. Liquid ejection across an expiration film upon hydraulic atomization of kerosene (a), (b) and biodiesel (c) at $G_A = 0$: (a) cylindrical nozzle, $G_F = 2.7$ g/s; (b), (c) annular nozzle, $G_F = 12.3$ g/s

Now we consider the dependence of the character of the fuel–air spray on the properties of the atomized liquids. Shown in Figs. 5 and 6 are pictures of the expiration of different fluids from cylindrical (Fig. 5) and annular (Fig. 6) nozzles with the same mass flow rate. The wave height above the level of the film depends apparently on the fluid viscosity because the relative shift of layers of the fuel becomes more difficult with increasing viscosity. Therefore, in Fig. 5a (water) one can easily see high wave formations. In Fig. 5b (kerosene) these formations have an appreciably lower height, and in Fig. 5c (a mixture of diesel and rapeseed oil), they are entirely absent.

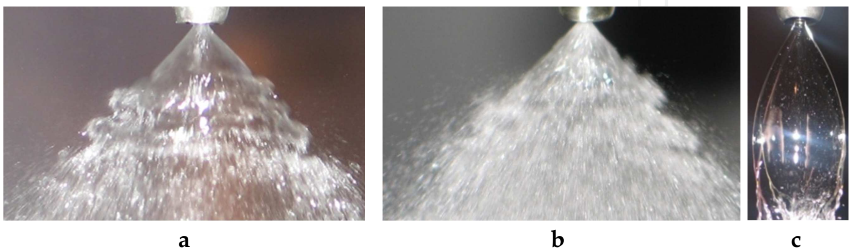

Figure 5. Comparison of the expiration of different liquids at the same mass flow through the cylindrical nozzle without air supply at $G_A = 0$, $G_F = 5$ g/s: (a) water, (b) kerosene, and (c) mixture of diesel with rapeseed oil (50%–50%)

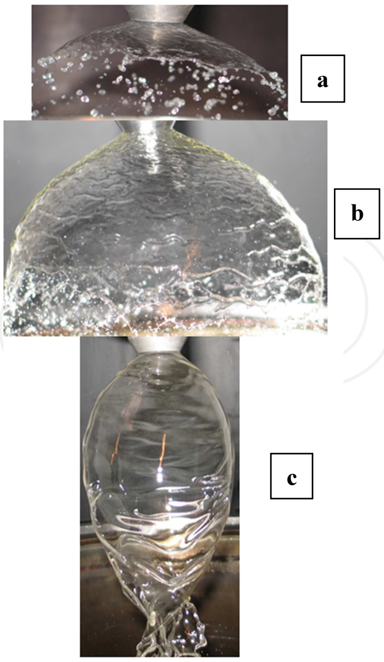

Figure 6. The same as in Fig. 5 in the case of an annular nozzle and $G_A = 0$, $G_F = 20$ g/s.

Figure 7. Expiration of kerosene through the centrifugal nozzle at $G_F = 5.5$ g/s: (a) without air supply ($G_A = 0$); (b) $G_A = 40$ g/s

Apart from the expiration velocity from the nozzle, the spray angle mainly depends on the viscosity of the fluid rather than on the surface tension (see Figs. 5, 6). The spray angle decreases with increasing viscosity. An analogous result stems from the experiments [17]. On the other hand, most likely, the remoteness of the point of the film disintegration from the output section of the nozzle depends mainly on the surface tension coefficient. As we can see from Fig. 6, the self-decay of kerosene and diesel-oil mix, with close surface tension coefficients occurs approximately on the same generator length of the film while the self-decay of water (having a considerably higher surface tension), occurs much earlier.

Having studied the waves formed on the surface of liquid films, one can assume the presence of similar effects in the case of mixed fuel–air flow. In reality, oscillations in the fuel concentration are usually observed upon pneumatic spraying. Their magnitude may change depending on the design of the sprayer unit, the injection velocity, and the properties of the ambient medium. In swirled flows in which the regions of the inverse fluid flows are formed, pulsations are observed on both the outer and inner borders of the burner. The formation of these pulsations is similar to the wave formation on the surface of the film (Fig. 2), but at the same time these effects are not related physically. Apparently, these formations occur behind the exit of the air nozzle due to sudden expansion and braking of the layer on the boundary with the external medium. Figure 7 demonstrates the independence of these vortexes on the waves formed on the surface of the film. Figure 7a shows the fuel spraying using a pressure swirl nozzle without air supply. The vortexes caused by the film of the fuel are visible only near the nozzle, but we do not see any pulsations of concentration elsewhere. Figure 7b shows the same injector with an external air swirler. We can easily see large wave formations propagating down through the flow and weakly correlating with the waves in the film.

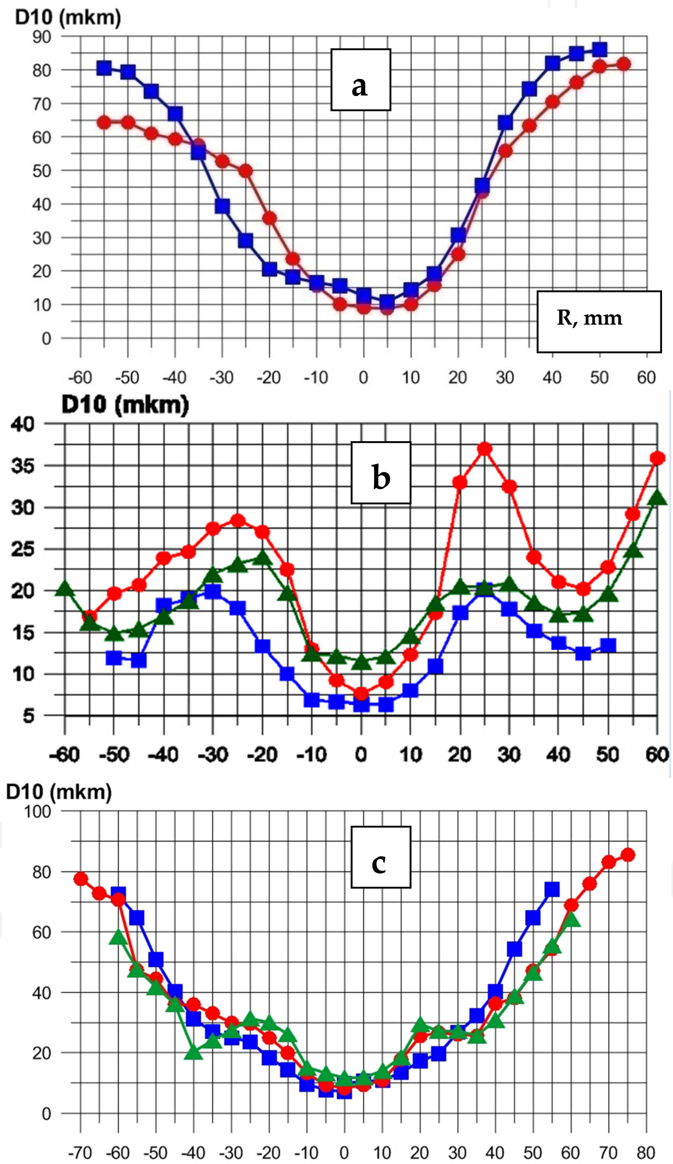

Figure 8. Linear distribution of the average droplet diameter over the burner diameter upon liquid atomization by three different methods: (a) centrifugal method, G_F = 5 g/s, G_A = 0; (b) centrifugal–pneumatic method, G_F = 5 g/s, G_A = 40 g/s; (c) pneumatic method, G_F = 20 g/s, G_A = 40 g/s; –● water, –■ kerosene, –▲ mixture of diesel with rapeseed oil (50%–50%)

Now we consider the impact of fluid properties and the related aforementioned phenomena on the dispersity of aerosol when using different methods of atomization (Figs. 8, 9). The first and most studied method of droplet atomization is that of centrifugation (hydraulic atomization). The liquid is fed through a near-axis pressure swirl nozzle without the external air flow (Figs. 8a, 9a). The average velocity of the fuel nozzle outlet of is 19–26 m/s depending on the type of liquid. The centrifugal–pneumatic method of atomization is shown in Figs. 8b and 9b. In this case, the average velocities of the fuel and air have the same order of magnitude. To implement centrifugal–pneumatic atomization, the fluid is fed through a pressure swirl nozzle with the same mass flow rate (5 g/s) as in the first case. Additionally, the air is fed through external swirlers with the total mass flow rate of 40 g/s. The average fuel velocity at the burner outlet is the same as in the first method (19–26 m/s) and on the order of 25 m/s for the velocity of air. In the third (pneumatic) atomization method (Figs. 8c, 9c), the injection velocity of the fluid is smaller than the velocity of air.

When implementing this method, a small part of liquid (3 g/s) is fed through the near-axis nozzle, while the main part (17 g/s) is fed through the annular airblast injector, and air velocity in this case is the same as in the second method. In this case, the average velocity is 3–4 m/s. The radial distribution of the diameter D_{10} of droplets is shown in Fig. 8, where D_{10} is the arithmetic mean of the size in an ensemble. This parameter determines the most probable size of droplets in the given region, and it can be used in predicting the engine wake-up mode: the greater the number of small droplets that enters the spark discharge zone, the simpler their evaporation and ignition.

Figure 9 shows the distribution of Sauter's mean diameter D_{32} of droplets - the ratio of the volume of a droplet to its surface area being averaged over the ensemble at a given point of space. This parameter is important when predicting the efficiency and homogeneity of the fuel burning.

As we can see from Figs. 8a and 9a, the viscosity of the liquid has a significant impact on the dispersity of droplets obtained by the centrifugal method of spraying. Thus, in the case of water having a surface tension three times higher, one can obtain droplets that are even smaller when compared with kerosene, which has a viscosity 1.9 times greater. In this case, a highly viscous mixture of diesel with rapeseed oil does not form waves on the surface of the film and is not sprayed at all (Fig. 5c). In the case of centrifugal–pneumatic spraying, as we can see from Fig. 8b, the most important role is played by the surface tension coefficient. The curves in Fig. 8b are arranged according to a consecutive increase in the surface tension and correspond to kerosene (bottom line), a mixture of diesel and rapeseed oil (middle line), and water (upper line). In Fig. 9b, we can note an insufficient secondary atomization of certain droplets with a large size in the flow of liquid with high viscosity. However, upon closer inspection, we can see that, at the locations of the maxima of concentration, the aforementioned dependence also takes place and it is violated only on the axis of the device near the zone of reverse flows due to insufficient intensity of the air flow. Further fragmentation of the drops of the viscous fluid near the separation zone can be done by aerating the root region of the fuel–air spray.

http://dx.doi.org/10.5772/59871

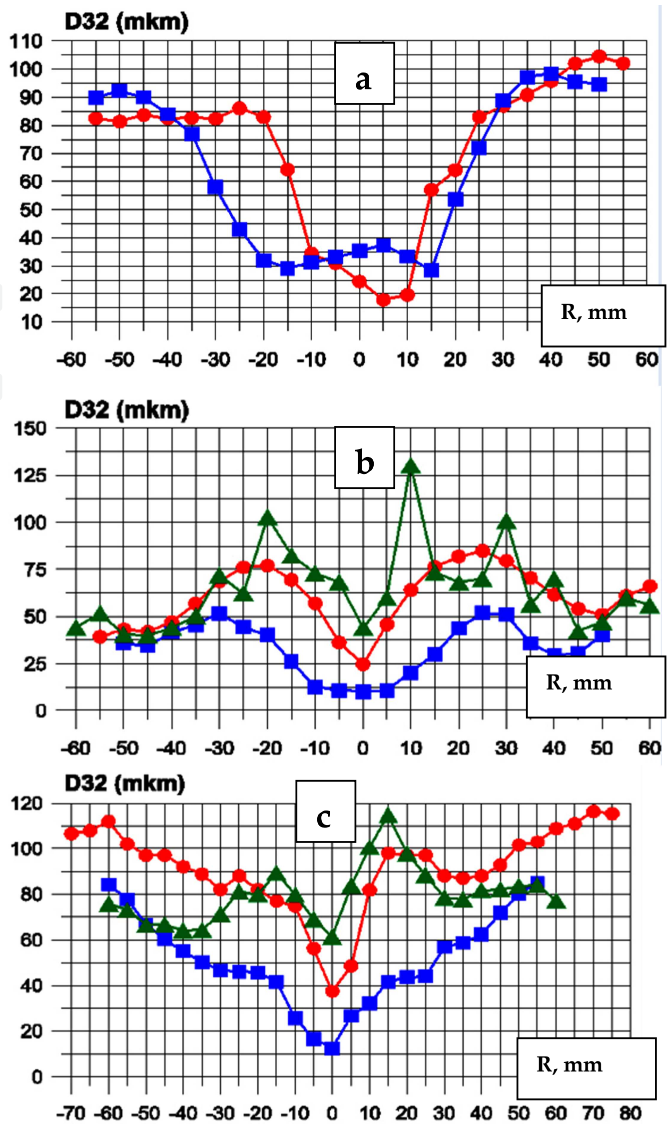

Figure 9. Distribution of the Sauter's drop diameters over the burner diameter upon liquid atomization by three different methods (designations are the same as in Fig. 8).

In the pneumatic method of spraying, as we can see from Fig. 8c, the influence of the properties of liquids on the linear size of droplets is nearly absent and all the curves merge into one. This parameter of aerosol is mainly determined by the air flow. Sauter's mean diameter of droplets (Fig. 9c) depends also on the surface tension coefficient. The influence of individual large drops is somewhat smoothened compared with the centrifugal–pneumatic method of spraying.

In the centrifugal–pneumatic method of spraying, the dispersity of droplets averaged over the whole section of the flambeau is the best. However, note that the ratio of the mass consumption of air to the mass flow rate of fuel (AAFR), which, in particular, determines the quality of spraying, equals 8 for this method and 2 in the case of the pneumatic method. Thus, in the case of low gas-turbine engine operating modes and high viscosity fuels like biodiesel or bio-kerosene, the centrifugal-pneumatic atomization method is optimal, while the pneumatic method is optimal for high operating modes.

3. The selection of mixed liquid fuel

For conducting the hot tests, ethanol and mixed biofuel on the basis of aviation kerosene (as most close relating to a turbine engine) have been chosen as alternative fuels. As one can see from Table 1, the combustion value of biofuels (especially ethanol) is significantly lower than that of fossil fuels. Furthermore, the viscosity of vegetable oils is ten times greater than the viscosity of the organic fuel. Therefore, for aircraft engines a blend of biofuels with conventional aviation fuels is more preferable then pure biofuels. At present, the use of industrially processed aviation biofuels in the Russian territory is not possible. Various versions of a percentage ratio of components of combustible mixtures on the basis of plant oil and ethanol (Table 2 and Fig. 10) have been investigated. Plant oil is necessary as surfactant for ethanol dissolution in the fuel. Aviation kerosene TS 1 or gasoline have been chosen as the main component of the mixture. The optimum ratio of components has been selected.

Figure 10. Photos of mixed fuels; signatures correspond to embodiments of the Table 2

	1	2	3	4	5
Kerosene TS-1	10%	30%	40%	50%	80%
Castor oil	10%	10%	20%	10%	10%
Ethanol	80%	60%	40%	40%	10%
	6	7	8		
Gasoline 95	80%	85%	10%		
Castor oil	10%				
Ethanol	10%	15%	90%		
	9	10	11		
Kerosene TS-1	40%	30%	50%		
Camelina sativa oil	20%	10%	10%		
Ethanol	40%	60%	40%		

Table 2. The embodiments of mixed liquid fuels

Analysis of the samples revealed that the use of different ratios of starting fuel, ethanol, and vegetable oil show results strikingly different from each other. It was possible to obtain well-blended homogeneous mixture only at certain narrow ranges of percentages of components. The embodiment 3 was chosen for further testing, as it showed the optimal ratio of components without settling on the bottom and without stratification. Variant 1, variants 6 and 7, and variant 8, which have also shown good mixing level, are notable for big maintenance of ethanol, kerosene or gasoline (up to 90 %). It is not beneficial in terms of the economic feasibility of introducing a new type of fuel.

For hot tests in the aviation combustion chamber, the mix in a ratio of 40% of kerosene TS-1, 20% of castor oil, and 40% of ethanol has been chosen as the most homogeneous and well mixed without any precipitations and stratifications. Its physical features are: $\varrho_F = 850$ kg/m^3, $\nu_F = 4.7 \times 10^{-6}$ m^2/s, and $\sigma_F = 27 \times 10^{-3}$ N/m.

4. Hot tests in aviation combustor.

Hot tests were performed at the Central Institute of Aviation Motors using a combusting chamber test rig. Fire tests of a burner with the low-emission aviation combustion chamber compartment have been conducted. Combustion chamber starting was conducted only on one pilot channel of a burner. Fuel mass flow rate ranged from 1 to 5.7 g/s. The part of the air arriving in the flame tube front passed through air swirlers of the burner. Thus, the centrifugal–pneumatic spraying was carried out, and as shown in the previous section, provided the best droplet dispersity. The kerosene TS-1, ethanol, and kerosene-ethanol-castor oil mixture were used as fuel. The operation mode corresponded to the altitude of an order of 2 km. The fixation of flame starting and blowout was carried out with the help of digital camera through a window at the liner outlet.

Test results are given in Figs. 11-20. The epures of the combustor's blowout characteristics at different excess air coefficients α_C and total air volume flow rates Q_C were obtained. Also the temperature fields behind an exit from the combustor in a pipe with a diameter of 110 mm have been taken out under various α_C.

Here α_C - the general excess air coefficient in the combustion chamber - the relation of total air mass flow rate passing through the chamber to the air flow rate was required theoretically for complete combustion of the fuel arriving at the same time in this chamber. Thus, $\alpha_C < 1$ means rich fuel-air mixture and $\alpha_C > 1$ means lean mixture.

The received blowout boundary line shows, that for conventional fuel (Figs. 11, 12), the combustor steadily works (the area within the curve) in the coefficient of air excess α_C range from 1 to 10 and till $Q_C = 0{,}4\ m^3/c$. The area boundary reaches satisfactory values on α_C, and comprehensible values on Q_C. The ignition domain (within the curve in Fig. 11) is sufficient on the square for assured firing of the combustion chamber.

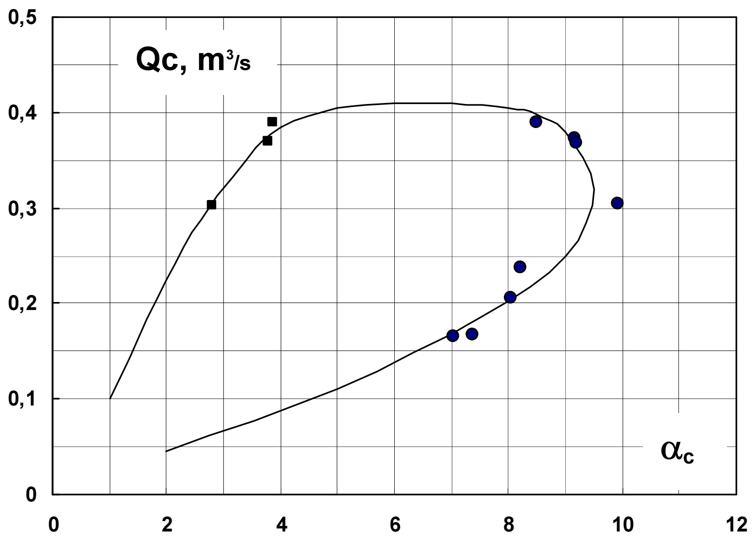

Figure 11.

Boundary lines of ignition and blowout in the combustion chamber compartment; fuel - kerosene TS-1; ● – lean blowout; ■ –rich blowout

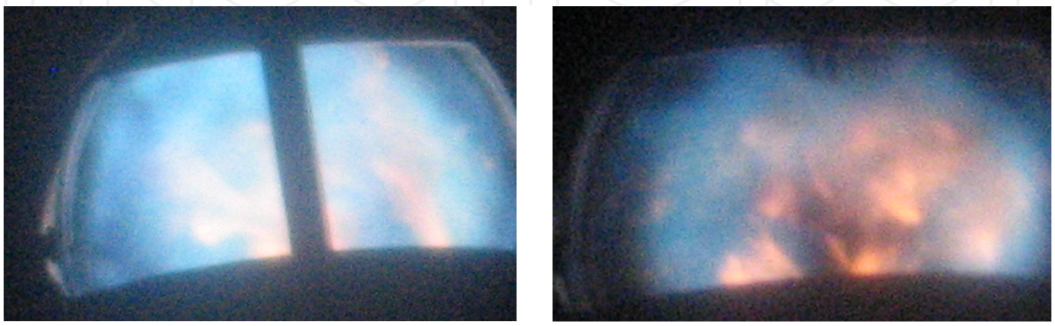

Figure 12. Flame photos at various α_C from wake-up to lean blowout (kerosene)

The radial temperature distribution at the combustor exit is shown in Fig. 13. The temperature field received has a symmetric appearance and a small non-uniformity on the value of the temperature - the minimum value differs from maximum on 50°C.

When using the ethanol (Figs. 14 - 16), lean blowout limit falls to $\alpha_C = 3$, and the combustor demonstrates stable operation only at major fuel flow rate (approximately $\alpha_C = 1.8$). This is due to the fact that alcohol is more volatile than the other liquid fuel, and thus, it will only burn before it can spread to a larger volume of flame front. The temperature reaches its maximum value with 300°C at $\alpha_C = 2.1$.

In view of the foregoing, the use of pure ethanol as an alternative type of aviation fuel is not possible, as a minimum, without the use of special fuel additives.

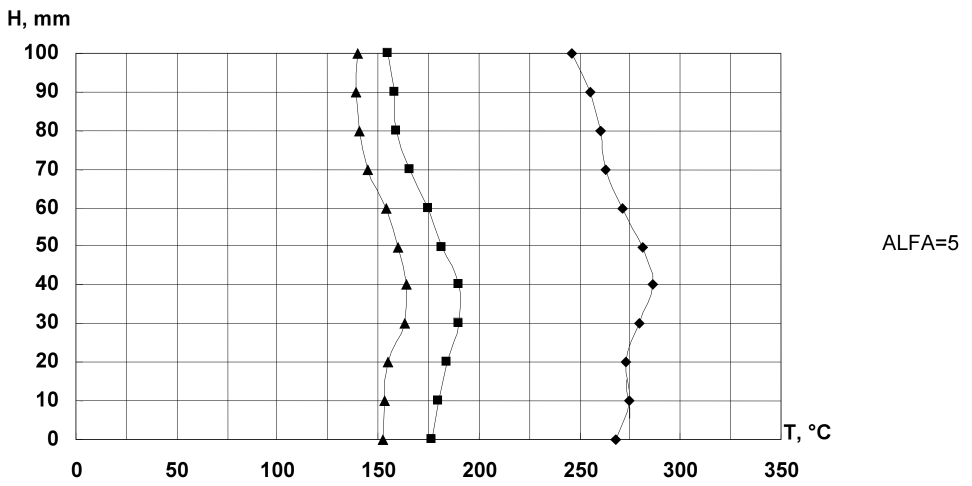

Figure 13. Temperature distributions along the height of the liner; ◆ - $\alpha_C = 3.5$, ■ - $\alpha_C = 5$, ▲ - $\alpha_C = 6.3$; fuel - kerosene TS-1; $Q_C = 0.3\ m^3/s$

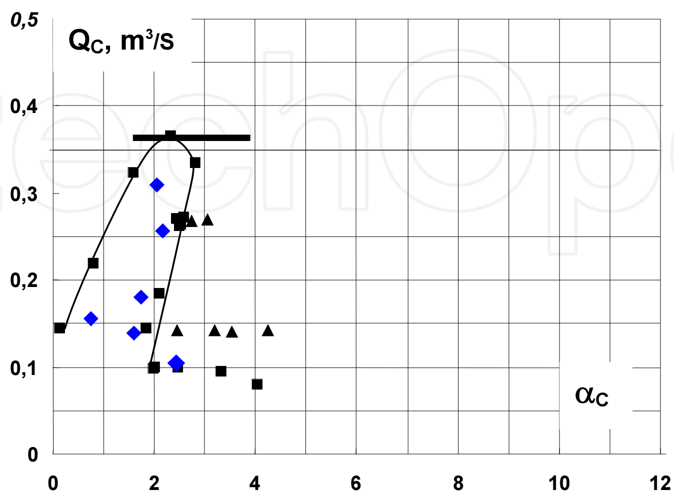

Figure 14. Boundary lines of ignition and blowout in the combustion chamber compartment; fuel - ethanol; ■ – blow-out, ◆ - combustor works, ▲ - combustor does not work

Figure 15. Flame photos at various α_C from wake-up to lean blowout (ethanol)

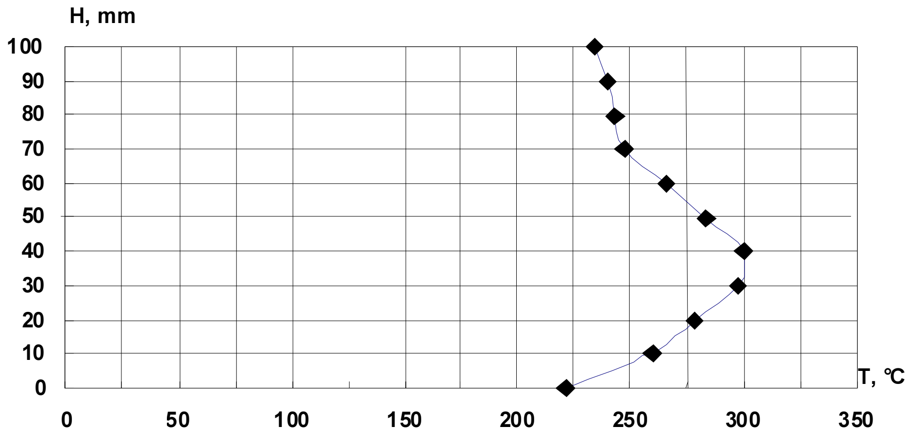

Figure 16. Temperature distribution along the height of the liner; fuel - ethanol; $\alpha_C = 2.1$; $Q_C = 0.21$ m^3/s

When using blended fuel (kerosene-ethanol-castor oil mixture), the combustor works better than at pure ethanol. Nevertheless, the lean blowout boundary is reduced from 10 to 6.5 at maximum volume flow rate conservation in comparison with kerosene (Figs. 11 and 17). The flame color (Fig. 18) changes while maintaining its overall structure due to the reduction of combusting efficiency and flame temperature and the increasing soot production. One can see from the comparison of Figs. 13 and 19 to 20 that when using blended fuel, it is possible to reach a maximum outlet flame temperature of 290°C only by increasing the mass of the injected fuel (α_C changes from 3.5 to 2.6).

Thus, biofuel application results in poor combustion stability characteristics for aircraft engines when compared with kerosene. For biofuel use, it is necessary to provide a number of actions for the modernization of conventional aviation combustion chambers. Main activities include the incorporation of artificial flame stabilizers into the design to preserve the stability limits of the combustor and the optimization of fuel injection system for the purpose of reducing fuel-air aerosol dispersity to maintain combustion efficiency.

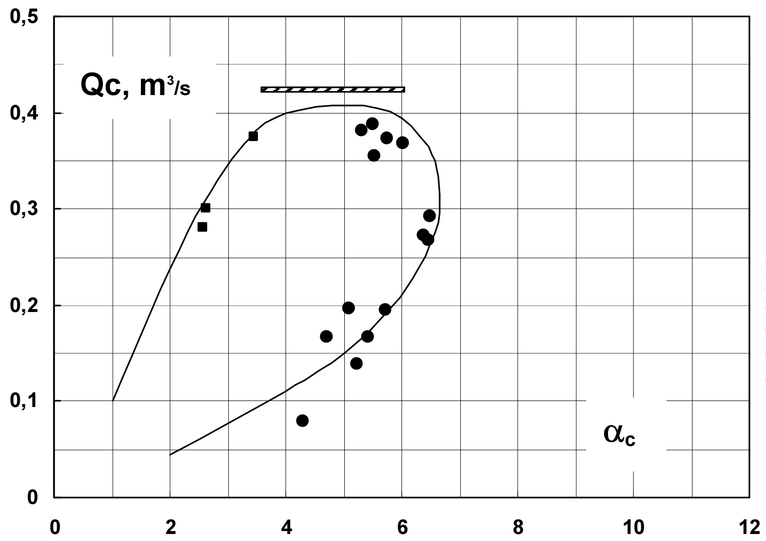

Figure 17. Boundary lines of ignition and blowout in the combustion chamber compartment; mixed fuel (the embodiment 3 from Table 2); ● – lean blowout; ■ –rich blowout

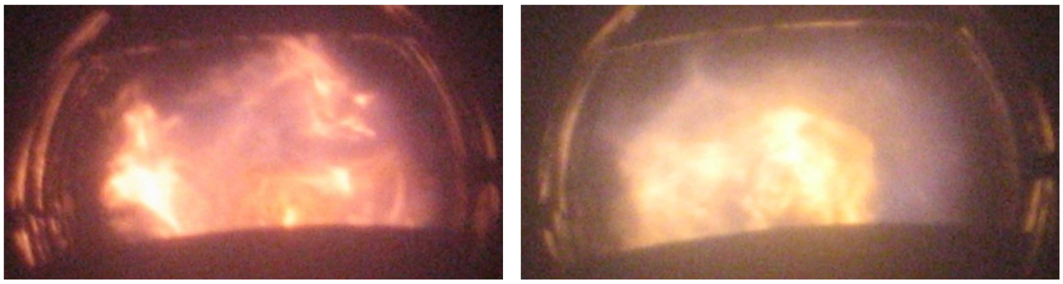

Figure 18. Flame photos at various α_C mixed fuel from wake-up to lean blowout; mixed fuel (the embodiment 3 from Table 2)

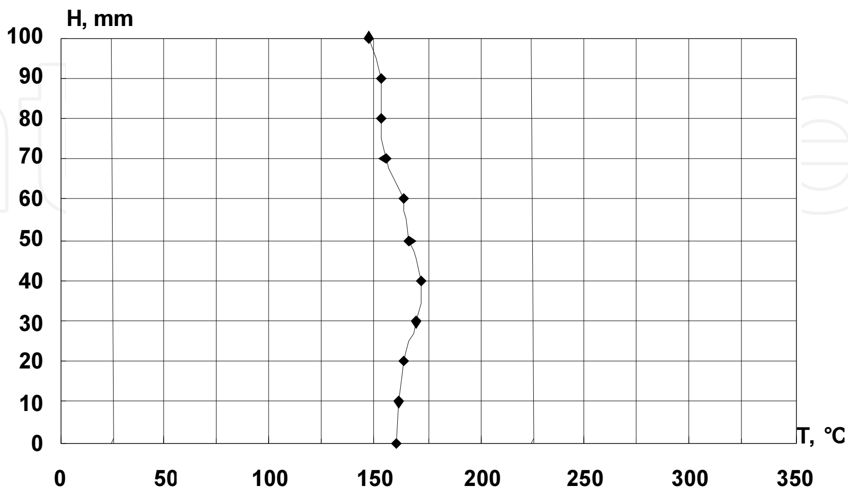

Figure 19. Temperature distribution along the height of the liner; $\alpha_C = 3.6$; mixed fuel (the embodiment 3 from Table 2); $Q_C = 0.29$ m^3/s

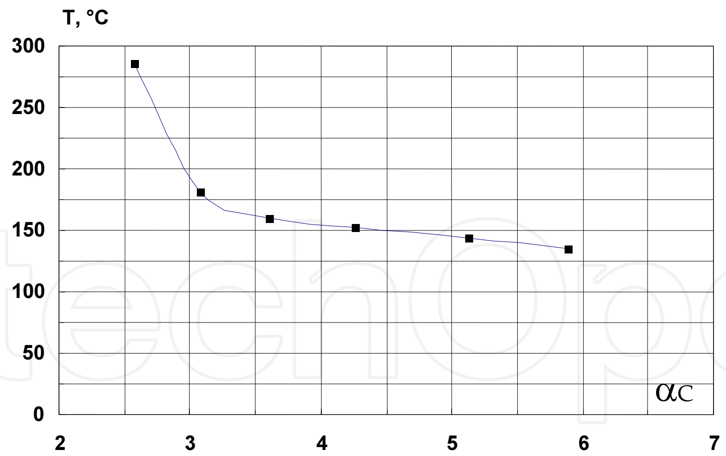

Figure 20. The dependence of axis temperature behind the combustor on excess air coefficient; mixed fuel (the embodiment 3 from Table 2)

5. Summary

An experimental study of the peculiarities of atomization of liquid fuels with different physical properties has been carried out. It has been shown that the spray angle upon hydraulic spraying is mainly determined by fluid viscosity, while remoteness of the point of the film decay from the exit section of the nozzle is determined by the surface tension coefficient. The effect of the properties of the liquid on the aerosol dispersity depends on the method of fluid crushing into droplets. In the case of the hydraulic atomization method without air supply, viscosity exerts the greatest impact on the dispersity of droplets. In the case of the centrifugal-pneumatic method (with the same order of magnitude of the velocity of liquid and air), the greatest impact is from the surface tension. In the pneumatic method of spraying, when the injection velocity of the fluid is lower than the velocity of air, the linear size of droplets is mainly determined by the air flow irrespective of the properties of the liquid, whereas Sauter's mean diameter depends also on the surface tension coefficient.

In the case of low gas-turbine engine operating modes and high viscosity fuels like biodiesel or biokerosene, the centrifugal-pneumatic atomization method is optimal, while the pneumatic method is optimal for high operating modes.

For conducting of hot tests in aviation combustor, 11 embodiments of mixed liquid fuels were proved. The mixture in a proportion of 40% of aviation kerosene, 20% of castor oil, 40% of ethanol had been chosen for the tests as the most uniform and well mixed, without deposition and stratification.

Fire tests of the compartment of aviation combustion chamber with fossil fuel (kerosene TS-1) have shown comprehensible characteristics. In particular, wide side-altars of the stable combustion, assured firing of the combustion chamber, with uniform enough field of gas temperature on exit.

http://dx.doi.org/10.5772/59871

The application of blended fuel (kerosene-ethanol-castor oil mixture) results in worse combustion stability characteristics for aircraft engines when compared with kerosene. For biofuel use, it is necessary to provide a number of actions for the modernization of conventional aviation combustion chambers.

Nomenclature

ν - kinematic viscosity, m^2/s

ϱ - density, kg/m^3

σ - surface tension coefficient, N/m

α- excess air coefficient

T – temperature, K

Q - air volume flow rate, m^3/s

G - mass flow rate, kg/s

D_{10} - droplet mean diameter, m

D_{32} - droplet mean Sauter diameter, m

Subscripts

A – air

C – combustion chamber

F - liquid fuel

Acknowledgements

This work was supported by the Russian Foundation for Basic Research, project No. 15-08-06293.

Author details

Anna Maiorova*, Aleksandr Vasil'ev and Oganes Chelebyan

*Address all correspondence to: majorova@ciam.ru

Central Institute of Aviation Motors named after P.I. Baranov, Russia

References

[1] Bernini E. Editor. Progress in Gas Turbine Performance. Rijeka: Intech. 2013. http://www.intechopen.com/books/progress- in-gas-turbine- performance (accessed 19 June 2013).

[2] Beginner's Guide to Aviation Biofuels, Red. 2. 2011.

[3] Boeing. 2013_environment report. http://www.boeing.com/aboutus/environment/environment_report_13

[4] https://www.klmtakescare.com/en/content/aruba-and-bonaire-on-biofuel

[5] http://www.biogas-rcb.ru/files/helpful/Biofuels-Market-Development-in-Russia-and-Worldwide.pdf.

[6] Marco Aurelio dos Santos Bernardes, Editor. Economic Effects of Biofuel Production. Rijeka: Intech. 2011.

[7] Marco Aurelio dos Santos Bernardes, Editor. Biofuel's Engineering Process technology. Rijeka: Intech. 2011.

[8] Manolis Gavaises (ed.). ILASS 2013. Proceedings of 25th European Conference on Liquid Atomization and Spray Systems, Chania, Greece, 1-4 September 2013.

[9] Charles K. Westbrook. Biofuels Combustion. Annual Review of Physical Chemistry. 2013. Vol. 64. pp 201-219.

[10] Russian State Standard 10227-86.

[11] Russian State Standard 305-82.

[12] European Standard EN 14214.

[13] J. Blin, C. Brunschwiga, A. Chapuisa, O. Changotadea, S. Sidibea, E. Noumia and P. Girard. Characteristics of vegetable oils for use as fuel in stationary diesel engines - towards specifications for a standard in West Africa. Renewable and Sustainable Energy Reviews. 2013; Vol. 22. pp. 580-597.

[14] Anna Maiorova, Aleksandr Sviridenkov, Valentin Tretyakov, Aleksandr Vasil'ev and Victor Yagodkin. THE DEVELOPMENT OF THE MULTI-FUEL BURNER In: Marco Aurelio dos Santos Bernardes (ed.). Economic Effects of Biofuel Production. Rijeka: Intech. 2011. pp. 281 - 298.

[15] A. Yu. Vasil'ev and A. I. Mayorova. Physical features of liquid atomization when using different methods of spraying. High Temperature, 2014, Vol. 52, No. 2, pp. 252–261. ISSN 0018_151X.

[16] A. Yu. Vasil'ev, A. I. Maiorova, A. A. Sviridenkov and V. I. Yagodkin. 2009. Patent of Russian Federation No. 86279.

[17] Soumik Mahapatra, Souvick Chatterjee, Swagata Shannigrahi, Achintya Mukhopadhyay and Swarnendu Sen. Experimental Investigation and Spray Characterization of Liquid Jet Atomization of Conventional Fuels and Liquid Bio-Fuels. ICLASS 2012, 12th Triennial International Conference on Liquid Atomization and Spray Systems, Heidelberg, Germany, September 2-6, 2012, proceedings. Contribution 1223b. ISBN 978-88-903712-1-9.

IntechOpen